Werk

Jahr: 1985
Kollektion: fid.geo
Signatur: 8 Z NAT 2148:58
Digitalisiert: Niedersächsische Staats- und Universitätsbibliothek Göttingen
Werk Id: PPN1015067948_0058
PURL: http://resolver.sub.uni-goettingen.de/purl?PPN1015067948_0058

LOG Id: LOG_0029
LOG Titel: Wave propagation in multilayered media: the effect of waveguides in oceanic and continental earth models
LOG Typ: article

Übergeordnetes Werk

Werk Id: PPN1015067948
PURL: http://resolver.sub.uni-goettingen.de/purl?PPN1015067948
OPAC: http://opac.sub.uni-goettingen.de/DB=1/PPN?PPN=1015067948

Contact

Niedersächsische Staats- und Universitätsbibliothek Göttingen
Georg-August-Universität Göttingen
Platz der Göttinger Sieben 1
37073 Göttingen
Germany
Email: gdz@sub.uni-goettingen.de

J Geophys (1985) 58:189–196

Journal of Geophysics

Wave propagation in multilayered media: the effect of waveguides in oceanic and continental Earth models

C. Chiaruttini[1], **G. Costa**[2], **and G.F. Panza**[1,2]

[1] Istituto di Geodesia e Geofisica, Università di Trieste, Italy
[2] International School for Advanced Studies, Trieste, Italy

Abstract. We investigate the effect of low-velocity waveguides on ground motion. The computation of eigenvalues and eigenfunctions of Rayleigh waves up to the frequency 10.0 Hz allows an analysis of the seismic response which is source independent. The main conclusions of this study are: (1) Extending the model to depths greater than that of the waveguides allows the exact computation of leaking modes. (2) A source in a layered structure generates *P* waves of higher frequency than *S* waves even if the structure is purely elastic. (3) At high frequencies (10.0 Hz) the modal components of *P* waves separate from those of *SV* waves. (4) Strong surface waves are generated by shallow sources in sedimentary basins, also at a source distance of a few tens of kilometres. These waves do not appear in structures without sediments. (5) The polarization of strong ground motion at the surface of low-velocity layers is mainly horizontal. (6) For oceanic models, the contribution of the sedimentary layers is separable from that of the water layer only at high frequencies.

Key words: Seismic waveguides – Sedimentary basins – Oceanic sediments – Rayleigh modes – Synthetic seismograms

Introduction

Low-velocity layers on top of an Earth structure form a waveguide which can trap seismic energy and propagate it to large distances even for media with very low Q. This kind of structure occurs frequently in seismological studies. Over large areas, the top of the continental crust is made of sedimentary rocks overlying a crystalline basement. The thickness of such sedimentary layers frequently ranges over a few kilometres and their fundamental eigenfrequencies may be as low as 0.1 Hz. On a smaller thickness scale, soft loose sediments often cover sedimentary rocks and constitute a sub-waveguide affecting frequencies of 1.0 Hz and higher.

In oceanic structures, the water layer and soft sediments on the oceanic floor constitute a waveguide affecting frequencies from 0.1 Hz to 10.0 Hz and more.

Seismic risk studies pay much attention to alluvial deposits, since it is well known that sites located on alluvium experience shaking which is stronger and lasts for a longer time than do sites located on rocks or stiff soils. This effect is named 'soil amplification', although this term is an improper one since no extra energy is supplied to the wave by the sediments. Most seismic risk oriented analyses of strong ground motion consider body waves only. Among body waves, *SH* waves are usually thought to be the ones bearing the greatest damaging potential. Examples of the importance of considering the whole wave field, including both surface and body waves, may be found in Hartzell et al. (1978) and in Johnson and Silva (1981). The strong motion recorded for the Imperial Valley earthquake in California on October 15, 1979, has a relevant surface-wave contribution (Brady et al. 1980).

Seismic exploration primarily makes use of body waves, although records of surface waves can be extremely useful in determining the presence and the gross properties of sedimentary basins. Tatham (1975) proposed the use of available seismograms as an easy and inexpensive procedure for the identification of sedimentary basins. More recently, Asten and Henstridge (1984) extended this proposal to the use of microseisms. Ebeniro et al. (1983) used surface waves, recorded during a refraction survey of the Texas coastal plain, to derive a smoothly varying vertical structure of the sedimentary cover down to a depth of 1.0 km. McMechan and Yedlin (1981) provide an example of the interest of using surface waves in marine seismic prospecting.

The computation of synthetic seismograms by normal mode superposition allows a complete insight into the response of a structure, both in the frequency and in the time domain (Panza 1985). This synthesis allows the exploitation of the greatest part of the signal since it includes surface waves and most of the body waves, thus providing much stronger constraints to the compatible crust models.

In the present paper we will investigate the response of a sedimentary continental and an oceanic structure by means of the computation and summation of Rayleigh modes. Frequencies up to 10.0 Hz will be considered.

The test models

The oceanic model considered is that of Harkrider (1970). The continental model is the crustal model of Fuis et al. (1982) for the Imperial Valley, overlying the upper-mantle model of Biswas and Knopoff (1974) for the western United States. The rest of the model down to a depth of 1,100 km is identical to the Harkrider (1970) continental shield structure. The lithosphere is 50 km thick and the Moho is at a depth of 25 km. The crust is made up of two homoge-

Offprint requests to: G.F. Panza

neous layers separated by a transition zone between 11.0 and 11.9 km in depth. They are overlain by 5.5 km of sedimentary rock characterized by *P*- and *S*-wave velocities with a constant gradient. Finally, 250 m of alluvial deposits constitute the topmost part of the structure.

The elastic and anelastic parameters of the two models are listed in Table 1 and plotted in Fig. 1 of the paper by Panza (1985) in this same issue of this journal.

The frequency-domain response up to 1.0 Hz

a) Oceanic structure

The phase-velocity spectrum, i.e. the dispersion curves, for the first 204 modes of the Rayleigh waves up to 1.0 Hz with step of 0.005 Hz has been computed for the oceanic structure (Fig. 1a).

For phase velocities higher than the asthenospheric channel *S*-wave velocity (about 4.3–4.4 km/s), the apparent continuity between adjacent modes, associated with the presence of different waveguides (Tolstoy and Usdin 1957; Tolstoy 1956; Deresiewicz and Mindlin 1955), makes it possible to easily differentiate the contribution of different mantle layers.

In Fig. 1a we can recognize the switching between crustal and channel waves for modes in the phase-velocity range 4.34–4.56 km/s (see Kovach and Anderson 1964; Schwab and Knopoff 1971; Panza et al. 1972). Beside these, sharp slope variations of nearly vertical trend in the dispersion curves are evident; for instance, at about 0.07 Hz, 0.20 Hz, 0.25 Hz, 0.75 Hz.

Eigenfunctions analysis (see later) shows that these families of modes correspond to waves which propagate essentially either in the sedimentary layer, or in the water layer, or in the sedimentary and water layers simultaneously. The above statement can be illustrated by comparing the spectra of a few elementary waveguides with the spectrum shown in Fig. 1a. Such elementary waveguides are made of only the shallowest layers, the boundary conditions being the free upper surface and a rigid substratum at the bottom. A comparison of the phase-velocity spectra of two elementary models, one formed by the water layer only and the other by the sedimentary layer only, showed that the correspondence with the mode-to-mode continuities present in the spectrum of the complete model is not satisfactory. On the other hand, the spectrum of an elementary model, formed by both the water and sedimentary layers, corresponds very nicely to the trend of the families of modes described in Fig. 1. The only portion of the spectrum, characterized by mode-to-mode continuation, which is not seen in the spectrum of the elementary structure (see dot-dashed line in Fig. 1a), corresponds to a crustal wave. This point will be considered in detail in a later section.

Considering the eigenfunctions of Fig. 2a, we see that point 2 in Fig. 1a reflects the properties of the sediments and the water layer. The depth intervals of the predominant portions of eigenfunctions corresponding to points 1 and 3 can similarly be shown to correspond to the water layer and sedimentary layer.

The points 4, 5 and 6, in terms of phase velocity, correspond to waves propagating mainly in the sedimentary layer. The eigenfunctions which correspond to points 4 and 6 (Fig. 2b and c), for both stress and displacement, are indeed concentrated in the sedimentary layer.

Points 7, 8, 9 and 10 follow the dot-dashed line of Fig. 1a. Eigenfunction sets, corresponding to these points, are all similar and only the one corresponding to point 9 is shown in Fig. 2d. Note that displacements and stresses are dominant in the sedimentary layer, but also penetrate significantly into the crustal layer below. It is, therefore, obvious that this spectrum characteristic, related to crustal waves, is not present in the spectra of the considered elementary models. The eigenfunctions calculated for points 7 and 8 have a remarkable energy concentration in the sedimentary and water layers. In fact point 7 is common to a mode of the elementary waveguide (water and sediment layers), whereas point 8 is close to a mode of the model made by the water layer only.

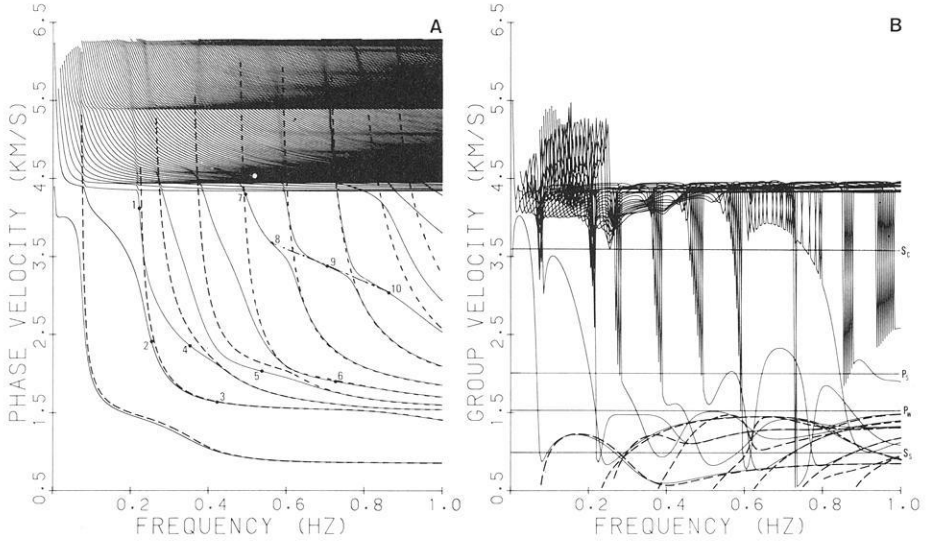

Fig. 1a and b. Dispersion curves for the oceanic model up to 1 Hz. **a** Phase velocities (*solid lines*) for the first 204 modes and **b** group velocities (*solid lines*) for the first 30 modes. On the figure are also shown the *P* wave velocity of the water layer (P_w), the *S* wave velocity of the crust (S_c) and the *P* wave and *S* wave velocities of the sedimentary layer, P_s and S_s, respectively. For the meaning of the numbers and of the dashed and dot-dashed lines, see text

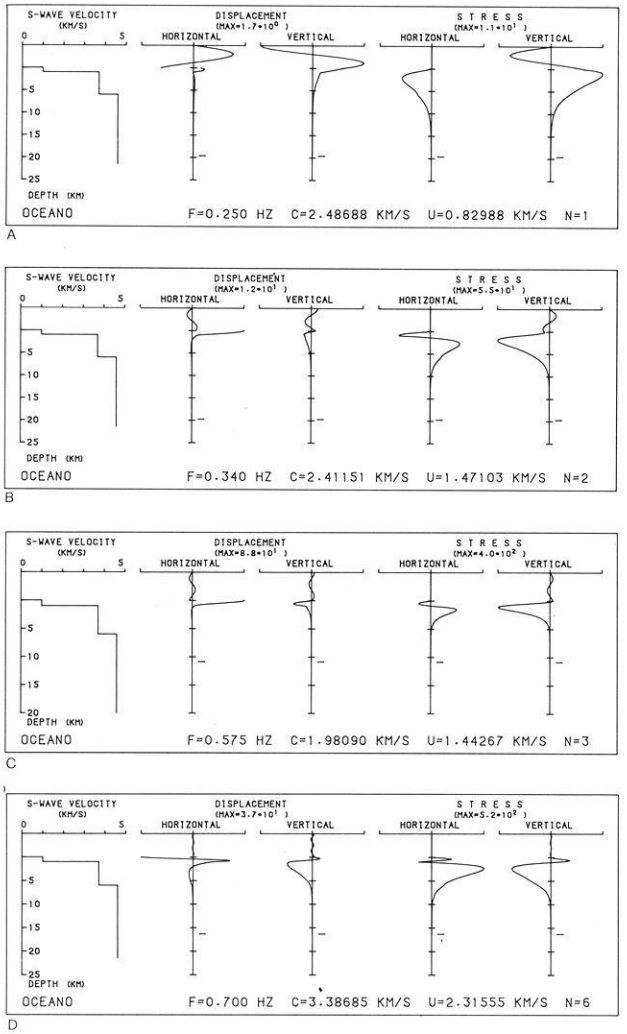

Fig. 2a–d. Eigenfunctions of the oceanic model. **a**, **b**, **c** and **d** correspond respectively to points 2, 6, 5 and 9 in Fig. 1a. *F* is frequency, *C* is phase velocity, *U* is group velocity, *N* is higher mode number

The main difference between the response of the elementary waveguides and the whole oceanic model is that, in the former case, the rigid boundary conditions at the bottom confine the energy in the one or two elastic layers considered. In the latter case, energy may reach greater depths. When the phase velocity is larger than the *S*-wave velocity just below the sediments, some energy always penetrates deeper. When this portion of energy is small compared to the total energy of the wave, the water and sediment layers act as a waveguide which leaks part of the energy to the underlying structure. The discrepancy between the elementary and the whole models is due to the absence in the elementary model of that part of the wave which penetrates deep into the crust and mantle.

The analysis of the group-velocity spectrum gives further confirmation of the interpretation given above. In order to avoid excessive close-packing of lines, the group-velocity spectrum for the first 30 modes only are shown in Fig. 1b, in which the dispersion curves of the water and sediments elementary waveguide are also indicated by dashed bold lines. For the group velocity of the other higher modes, see Fig. 5b–d of Panza (1985).

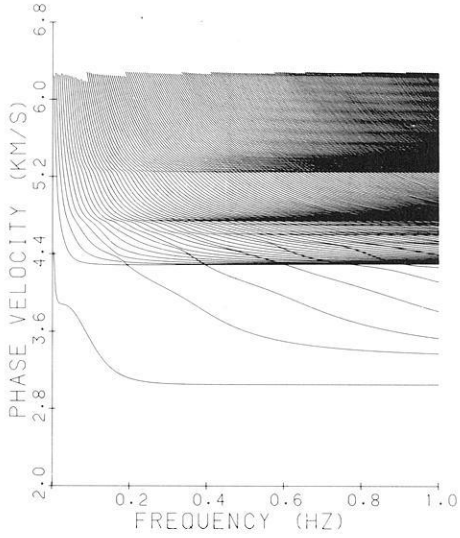

Fig. 3. Phase-velocity spectrum of the model IMP2. First 209 modes

Also in the group-velocity spectrum, the modes are grouped in a way which reflects the main layering of the *S*-wave and *P*-wave velocities. Information for the deeper layers, and higher velocities, is not present because only the first 30 modes have been plotted.

b) Continental structure

A concise description of the response of this model for frequencies as high as 1.0 Hz is given by Panza (1985). In this paper, we will focus our attention on the families of waves formed by the mode-to-mode continuation of the steep segments of the phase-velocity dispersion curves (Panza 1985, Fig. 2) in the frequency ranges 0.08–0.13 Hz, 0.30–0.50 Hz, 0.68–0.95 Hz. A fourth family is present in the range 0.88–1.00 Hz, but is not seen in the figure due to the limited resolution of the drawing.

As a first proof of the sedimentary nature of such waves, let us compare Fig. 2 of Panza (1985) with the phase-velocity spectrum in Fig. 3, where such families of waves do not appear either in the domain of mantle or of crustal velocities. The model IMP2 is similar to IMP1, except that the sediments are replaced by a homogeneous layer of the same thickness as the sediments which has the same properties as the bedrock. Removing the sediments results in a simplification of the spectrum in the crustal wave domain for velocities smaller than 4.3 km/s. The spectrum of the group velocities leads to the same conclusions.

Figure 4 shows examples of eigenfunctions. The wave in Fig. 4a and b belongs to the second of the families we are investigating. One can see that the motion is almost totally confined to the sediments, thus confirming our earlier arguments. In contrast, Fig. 4c shows the eigenfunctions of a wave which samples the crust and the mantle down to a depth of 450 km. The wave in Fig. 4a and b has a group velocity of about 3.0 km/s, and is of dominantly compressional nature as can be seen by the larger values of the vertical (i.e. compressional) stress with respect to the horizontal (i.e. shearing) stress. This argument is confirmed by the value of the group velocity which is in the range of the *P*-wave velocities in the sedimentary cover.

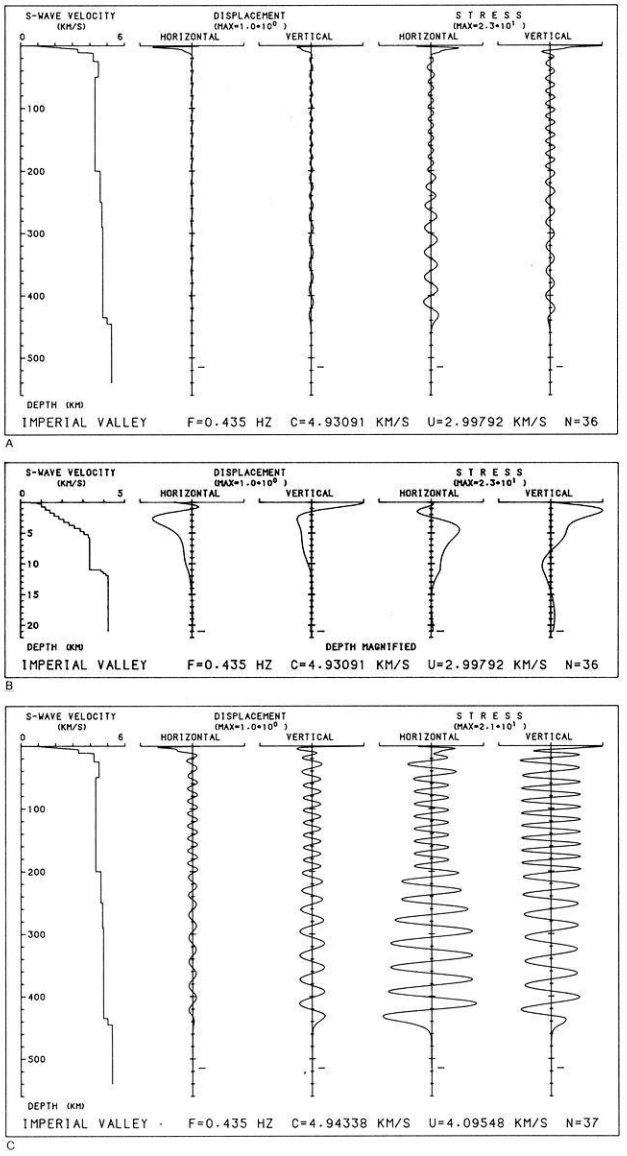

Fig. 4a–c. Eigenfunctions of the continental model IMP1. **a** sedimentary wave; **b** blow-up of the lithospheric part of the same wave; **c** non-sedimentary wave. F is frequency, C is phase velocity, U is group velocity, N is higher mode number

Such a wave is thus mainly a compressional sedimentary wave which is coupled with a smaller-amplitude mantle wave of mainly shearing nature. Waves of this type arise from the predominance of the compressional potential over the shearing potential and are the modal components of the sedimentary P waves. In order to be synthesized, they require a model which includes a mantle.

The frequency-domain response up to 10.0 Hz

A deeper insight into the response of the test models is given by the extension of the above computations to 10.0 Hz. In this case we simplify the structure by retaining only the lithosphere. This reduction in layers saves a large amount of computer time since it avoids the computation of nearly 2000 mantle modes.

a) Oceanic structure

From the previous section it follows that the contributions, in the phase-velocity spectra calculated up to 1.0 Hz, of two layers with low acoustic impedance – in this particular case the water layer and the sedimentary layer – are not distinguishable. To resolve these layers it is necessary to calculate the phase and group velocities at higher frequencies (Fig. 5a and b). For frequencies higher than 1.0–1.5 Hz, the apparent horizontal continuity from mode to mode corresponds to the stratification of the structure. In fact the nearly horizontal sections of the numerous families of waves correspond to the velocity of S waves propagating in the crustal layer (3.6 km/s), to that of the P waves propagating in the water layer (1.52 km/s) and to that of the S waves propagating in the sedimentary layer (1.0 km/s), when progressively lower values of the phase velocity are examined. In this frequency band the three superficial layers of the oceanic structure behave as individual waveguides and their contributions are easily separable. In particular, it is very interesting to observe the apparent continuity from mode to mode in relation with the P wave velocity in the water layer, which introduces a remarkable grouping of modes.

It is wort noting that the number of modes for the 10.0-Hz spectrum is strictly related to the water thickness. In fact, if the water thickness is reduced to 2.0 km, the spectrum exhibits only 68 modes. On the contrary, calculating the spectrum up to 1.0 Hz with 2.0 km of water, the number of modes remains greater than 200. Furthermore, it is remarkable that the continuity from mode to mode, in correspondence with the P wave velocity (2.1 km/s) of the sedimentary layer (Fig. 5a), corresponds to that barely apparent for the first three higher modes of the spectrum calculated up to 1.0 Hz (Fig. 1a). The portion of the spectrum between the S wave velocity of the crustal layer and the P wave velocity of the sedimentary layer is characterized by two families of modes, whose trends are marked by a thick solid and a thick dashed line in Fig. 5a. They correspond to sedimentary and water waves respectively, as we will show in analysing the eigenfunctions.

The eigenfunctions calculated at the points 1, 2, 3 and 4 (solid line trend), show that these are sedimentary waves. In fact, nearly all the stresses and the displacements are concentrated in the sedimentary layer. They are all very similar and the one corresponding to point 4 is shown in Fig. 6a. The eigenfunctions in Fig. 6b and c have been calculated at points 5 and 6 to interpret the wave families with the trend marked by the dashed line in Fig. 5a. They show that the energy is concentrated in the water layer and in a little part in the sediments. If the phase-velocity spectrum of the waveguide formed by the water layer only on top of a rigid substratum is calculated, it may be seen that this spectrum can be juxtaposed, in a large part, to the families of waves indicated by the dashed line trend.

The eigenfunctions corresponding to the mode grouping close to the P wave velocity of the sedimentary layer (points 7, 8 and 9) show that they are mainly sedimentary compressional waves, as can be deduced by the dominant vertical (i.e. compressional) stress. It is very interesting to note here also that, in the same sedimentary layer, two waves of different vertical wavelength are present. The long-wavelength component is associated with the P wave propagating in the sediments, while the component of short wavelength corresponds to the sedimentary S wave. It is interesting

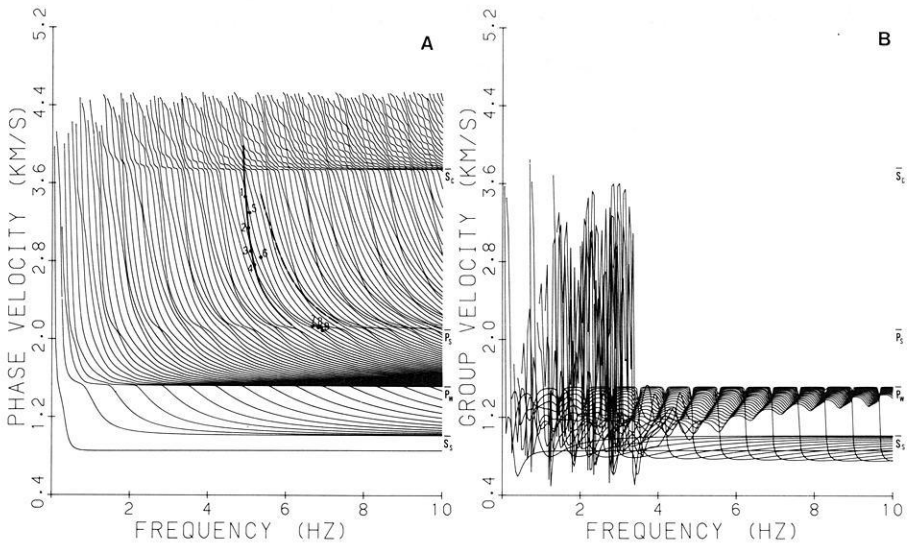

Fig. 5a and b. Dispersion curves for the oceanic model up to 10.0 Hz. **a** Phase velocities for the first 106 modes, **b** group velocities for the first 30 modes. On the figure are also shown the P wave velocity of the water layer (P_w), the S wave velocity of the crust (S_c) and the P wave and S wave velocities of the sedimentary layer, P_s and S_s, respectively. For the meaning of the numbers and the thick lines, see text

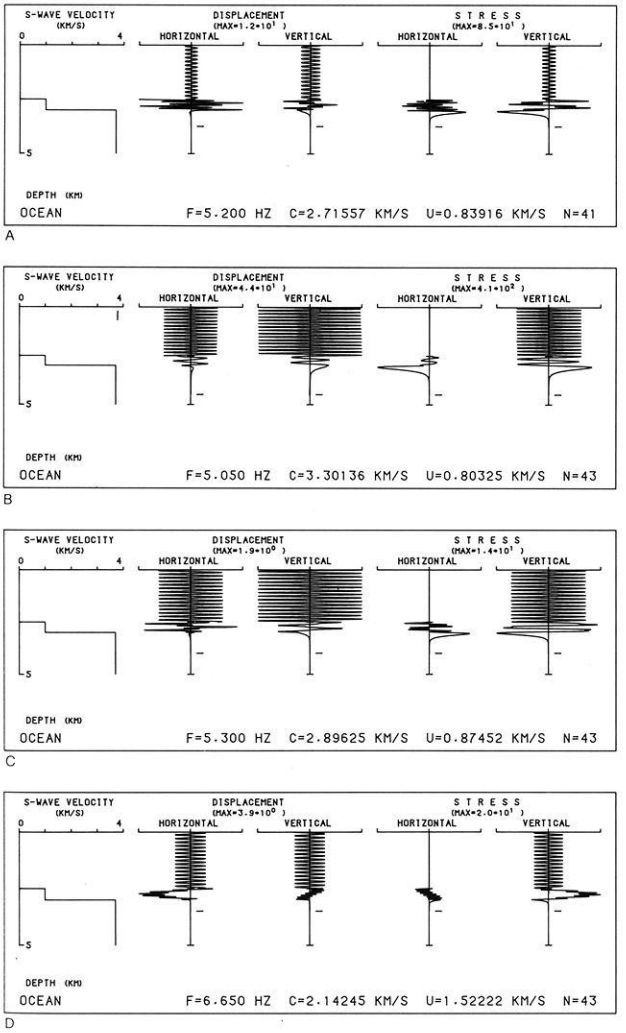

Fig. 6a–d. Eigenfunctions of the oceanic model. **a**, **b**, **c** and **d** correspond respectively to points 4, 5, 6 and 7 in Fig. 5a. *Symbols* in the plot are as for Fig. 2

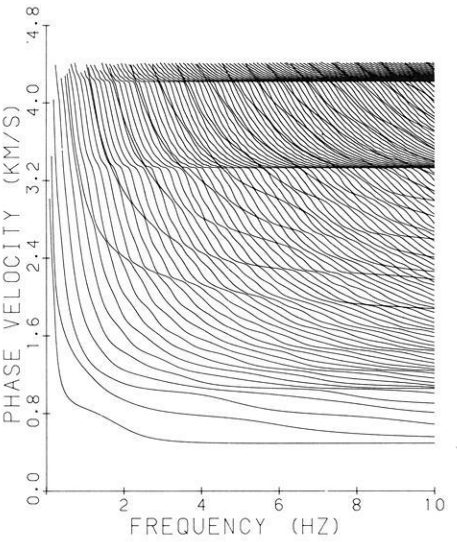

Fig. 7. Phase-velocity spectrum of the continental model IMP1 up to 10.0 Hz. First 118 modes

to note also, in these points, that the P wave propagating in sediments carries along a significant component of the water wave.

b) Continental structure

In the phase-velocity spectrum of model IMP1 (Fig. 7) we can see the traces of the two crustal layers having a velocity of 3.32 km/s and 4.21 km/s, respectively. In the bottom of the figure, we see that the modes are sparser for velocities smaller than 1.0 km/s. This value corresponds to the velocity of the top of the sedimentary rock layer, velocities from 1.0 km/s down to 0.5 km/s belonging to the thin layers of alluvial deposits.

Following the mode-to-mode continuity of the dispersion curves across the near-osculation points, we recognize

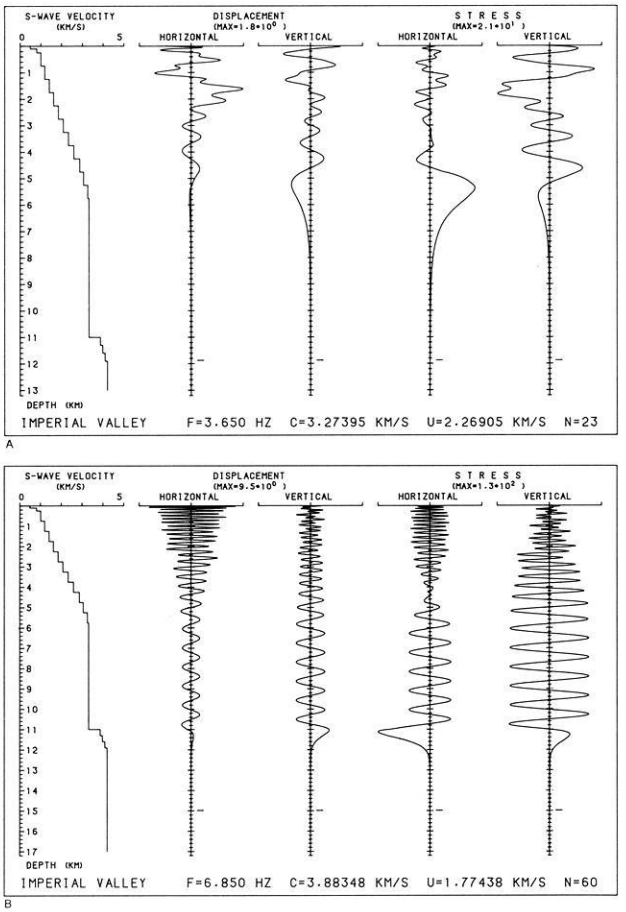

Fig. 8a and b. Eigenfunctions of the continental model IMP1. **a** sedimentary wave, **b** upper crustal wave. *Symbols* in the plot are as for Fig. 2

two sets of curves: one formed by a large number of closely spaced lines which inflect in correspondence to the main discontinuities in the S wave velocities, the other formed by 17 curves, more widely separated from each other and all contained above the velocity of 1.9 km/s. In analogy with what has been observed in the ocean case, thinking in terms of rays, the former are the modal components of the crustal and sedimentary S waves and the latter are the modal components of the sedimentary P waves. Figure 8 shows two examples of eigenfunctions. Figure 8a shows a wave in which the presence of both compressional and shearing elastic potentials are evident; a small-amplitude and small-vertical-wavelength S wave is coupled with a large-amplitude and large-vertical-wavelength P wave. The wave in the eigenfunction of Fig. 8b can be identified as an S wave since it uniformly samples the upper crust with a dominant wavenumber k practically coincident with ω/V_s.

Time-domain responses

a) Oceanic structure

Two examples of the radial component of motion up to 1.0 Hz (Fig. 9a) and up to 10.0 Hz (Fig. 9b) were calculated utilizing the spectra analysed before and following the formalism given by Panza (1985). The source for the two seismograms has been placed at a depth of 1.0 km, at the interface between the sedimentary and the crustal layers. The characteristics of the double-couple source considered are: dip = 90°, rake = 0°; the receiver is placed at a distance of 50 km and at an azimuth of 225° with respect to the fault strike.

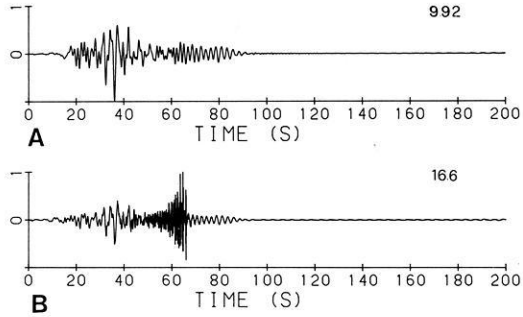

Fig. 9a and b. Example of seismograms for the oceanic model calculated up to 1.0 Hz (**a**) and up to 10.0 Hz (**b**) for the same source. The number above each seismogram is the peak displacement in centimetres for a seismic moment of 10^{18} Nm

If the scale factors of the two seismograms are properly chosen, and the seismograms are compared, it is possible to see the nearly perfect correspondence between the two signals up to 45 s and after 65 s. In the time interval between these values a signal of high frequency is present (Fig. 9b); it is characterized by a large amplitude, nearly 1.7 times the maximum amplitude of the 1.0-Hz seismogram. This signal can be associated with multiple reflections in the sedimentary layer. In fact, the arrival time of this signal is about 50–60 s, which corresponds to a group velocity of 0.8–1.0 km/s. Such a velocity corresponds, in the group-velocity spectra, to the mode grouping around the S wave velocity of the sedimentary layer.

Thus, the seismogram calculated for 10.0 Hz carries some information regarding the superficial sedimentary layer which is not present in the seismogram calculated up to 1.0 Hz.

b) Continental structure

As examples of time-domain responses, consider the seismograms of Fig. 10. They are computed assuming the same focal parameters and source-to-receiver geometry for the two earth models. The source is a strike-slip fault on a sub-vertical plane at a depth of 2.75 km (i.e. in the sediments in the case of the IMP1 model). The expected trapping of energy in the sediments is apparent and results in much longer signals with many crustal reverberations and long surface-wave trains in the case of the IMP1 model. Surface waves have the same maximum amplitude as the body waves. At 1.0 Hz, the peak vertical displacement of the model IMP1 is slightly larger than that of the model IMP2. The wave train arriving after 60 s has a frequency of about 0.28 Hz and a velocity of 0.75 km/s; it is due to the excitation of the fundamental mode. The earlier train arriving around 40 s has a velocity of 1.32 km/s and a frequency of about 0.20 Hz, which corresponds to the stationary phase of the minimum of the first higher mode (see Panza 1985, Fig. 4a). The two distinct large arrivals in the IMP2 seismograms at 1.0 Hz (Fig. 10b and d) are the direct P and S waves.

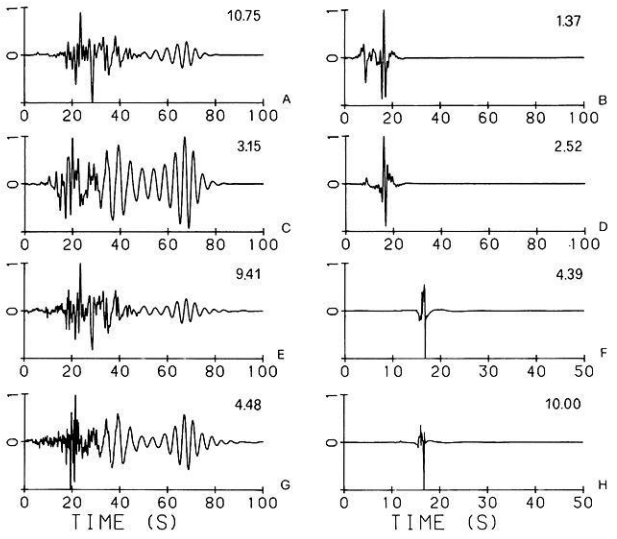

Fig. 10a–h. Examples of synthetic seismograms for the continental models. Source parameters are: dip 85°, rake 180°, depth 2.75 km, seismic moment 10^{18} Nm. The distance of the receiver is 50 km and its azimuth with respect to the fault strike is 150°. **a** Model IMP1, 1.0 Hz, horizontal component; **b** model IMP2, 1.0 Hz, horizontal component; **c** model IMP1, 1.0 Hz, vertical component; **d** model IMP2, 1.0 Hz, vertical component; **e** model IMP1, 10.0 Hz, horizontal component; **f** model IMP2, 10.0 Hz, horizontal component; **g** model IMP1, 10.0 Hz, vertical component; **h** model IMP2, 10.0 Hz, vertical component. The number above each seismogram is the peak displacement in centimetres

In Fig. 10 we see that the sediments make the radial motion 2–3.4 times as high as the vertical one. Note that no *SH* waves are present. Nevertheless, the surface motion of model IMP1 is predominantly horizontal. This is due to the ellipticity (i.e. the ratio of the radial to vertical amplitude of motion at the surface) which, in the presence of low-velocity surface layers, assumes large absolute values over a large part of the spectrum (see Panza 1985, Fig. 9a–d). This effect of slow superficial layers has already been pointed out by Mooney and Bolt (1966) – see, in particular, their Figs. 11–16.

Comparing the seismogram for the model IMP1 at 1.0 Hz (Fig. 10a and c) and at 10.0 Hz (Fig. 10e and g), we see that the long-period late parts of the seismograms are the same in both cases and that the first parts are similar, except for the obviously larger frequency content of Fig. 10e and g. The radial components have nearly the same amplitude, whereas strong high-frequency phases at about 20 s increase the amplitude of the vertical component of the 10 Hz seismogram by 40%. This is due to the simultaneous arrival of both *S* waves reflected at the 11-km and at the 25-km discontinuities, which constructively interfere at a source distance of 50 km.

In the case of model IMP2, the 10.0-Hz seismogram (Fig. 10f and h) has a peak amplitude about four times larger than the one at 1.0 Hz (Fig. 10b and d) due to high-frequency pulses which are efficiently transmitted by the high-Q layers of this model. The main difference is the absence of the direct *P* wave in the 10.0-Hz seismogram. It cannot be synthesized in this case since the half-space of the 10.0-Hz model has a shear-wave velocity of 4.5 km/s, which is less than the *P* wave velocity in the uppermost layer (see also Panza 1985). On the contrary, in the oceanic 10.0-Hz seismogram, sedimentary *P* waves are present because of their low velocity in the sediments (2.1 km/s) compared with the *S*-wave velocity of the half-space (4.61 km/s).

The frequency of P and S waves

It is generally assumed in seismology that the spectra of *S* and *P* waves at the source have the same shape and that the observation of higher frequency in *P* waves is explained by a larger attenuation of *S* waves in their travel through the earth. Figure 7 shows that the sedimentary *S* waves (bottom of the figure) reach their horizontal asymptote at frequencies smaller than the sedimentary *P* waves do. Since the flat portions of dispersion curves correspond very closely to sub-horizontal rays of practically non-dispersed body waves, it follows that the earth structure responds to any excitation with higher frequencies in *P* waves than in *S* waves. This fact is not surprising if we think that a layered structure is essentially a set of coupled oscillators and that the larger velocity of *P* waves implies that they have resonant frequencies which are larger than those of *S* waves. Note that this conclusion is valid also for purely elastic structures, since the Earth's anelasticity in general does not affect the first four digits of the phase velocity. The same conclusion could be drawn from the spectrum of the oceanic model (Fig. 1a). This remark of course deserves a more detailed discussion than is possible here. Nevertheless, we think it is worth a mention here for the relevance it has in the measurement of Q in the Earth.

Conclusions

We have shown that the application of the algorithm presented by Panza (1985) to earth models including low-impedance superficial waveguides, both in continental and oceanic environment, permits the synthesis, in a mathematically simple way, of all types of guided waves. Besides surface waves, they include some *P* waves and practically all *S* waves, thus allowing the full synthesis of the wave phases of shallow sources recorded up to epicentral distances of about 100 km.

Until now, leaking mode theory (Phinney 1961) has been used to compute the waves which almost totally propagate in low-impedance waveguides and which have a small fraction of their energy travelling in the substratum. In our approach they are computed as any other higher mode, thus avoiding all the mathematical complexity of the leaking mode theory.

The late arrivals of the guided waves may be synthesized considering lithospheric models only. To obtain also the early *P* wave arrivals, it is necessary to consider an earth model which is thick enough to include all layers having *S* wave velocities smaller than the *P* wave velocity in the waveguide. This means that in most cases the model should extend to a depth of 1,000 km.

The layering of the earth has the consequence that the Fourier spectrum of an *S* wave extends to frequencies lower than that of a *P* wave, even for purely elastic structures. This fact should be considered when measuring the anelasticity of the Earth.

In the case that the waveguide is composed of two layers which do not differ greatly in impedance, as in the case of the oceanic model, it is necessary to perform high-frequency computations in order to separate the waves propa-

gating in the two individual layers. The presence of significant lateral heterogeneities will of course invalidate the process of modelling by flat layers. There do appear to be regions, however, such as portions of ocean basins, where approximate lateral homogeneity persists for at least several tens of kilometres. The recording of short-period waves like those already illustrated in the seismogram of Fig. 9b could be used as evidence for the presence of undisturbed sedimentary deposits.

Finally, we have shown that in the case of low-impedence waveguides the particle motion of Rayleigh waves at the surface becomes predominantly horizontal. This part of the wave field should also be considered in seismic risk studies, especially since the radiation patterns of Love and Rayleigh waves are generally complementary in azimuth.

Acknowledgements. We thank Prof. B.J. Mitchell for critically reading the manuscript. Thanks are due to Mrs. I. Galante for the typing of the manuscript and to Mr. M. Gergolet and Mr. S. Zidarich for their help in elaborating the diagrams.

This research has been performed with the financial support of CNR (grants 83.02248 and 83.02432) and MPI (40% and 60%).

References

Asten, M.W., Henstridge, S.D.: Array estimators and the use of microseisms for reconnaissance of sedimentary basins. Geophysics **49**, 1828–1837, 1984

Biswas, N.N., Knopoff, L.: The structure of the upper mantle under the United States from the dispersion of Rayleigh waves. Geophys. J.R. Astron. Soc. **36**, 515–539, 1974

Brady, A.G., Perez, V., Mork, P.N.: The Imperial Valley earthquake, October 15, 1979, digitization and processing of accelerograph records. U. S. Geol. Surv., Open-File Rept. 80–703, 309 pp. 1980

Deresiewicz, H., Mindlin, R.D.: Axially symmetric flexural vibrations of a circular disk. J. Appl. Mech. **22**, 86–88, 1985

Ebeniro, J., Wilson, C.R., Dorman, J.: Propagation of dispersed compressional and Rayleigh waves on the Texas coastal plain. Geophysics **48**, 27–35, 1983

Fuis, G.S., Mooney, W.D., Healey, J.H., McMechan, G.A., Lutter, W.S.: Crustal structure of the Imperial Valley region. U. S. Geol. Surv. Prof. Paper 1254, 25–49, 1982

Harkrider, D.G.: Surface waves in multilayered elastic media. Part II. Higher mode spectra and spectral ratios from point sources in plane layered elastic models. Bull. Seismol. Soc. Am. **60**, 1937–1987, 1970

Hartzell, S.H., Brune, J.N., Prince, J.: The October 6, 1974 Acapulco earthquake: an example of the importance of short period surface waves in strong ground motion. Bull. Seismol. Soc. Am. **68**, 1663–1677, 1978

Johnson, L.R., Silva, W.: The effects of unconsolidated sediments upon the ground motion during local earthquakes. Bull. Seismol. Soc. Am. **71**, 127–142, 1981

Kovach, R.L., Anderson, D.L.: Higher mode surface waves and their bearing on the structure of the earth's mantle. Bull. Seismol. Soc. Am. **54**, 161–182, 1964

McMechan, G.A., Yedlin, M.J.: Analysis of dispersive waves by wave field transformation. Geophysics **46**, 869–874, 1981

Mooney, H.M., Bolt, B.A.: Dispersive characteristics of the first three Rayleigh modes for a single surface layer. Bull. Seismol. Soc. Am. **56**, 43–67, 1966

Panza, G.F.: Synthetic seismograms: the Rayleigh waves modal summation. J. Geophys. 1985

Panza, G.F., Schwab, F., Knopoff, L.: Channel and crustal Rayleigh waves. Geophys. J. R. Astron. Soc. **30**, 273–280, 1972

Phinney, R.A.: Leaking modes in the crustal wave-guide. 1. The oceanic Pl wave. J. Geophys. Res. **66**, 1445–1469, 1961

Schwab, F., Knopoff, L.: Surface waves on multilayered anelastic media. Bull. Seismol. Soc. Am. **61**, 893–912, 1971

Tatham, R.H.: Surface-wave dispersion applied to the detection of sedimentary basins. Geophysics **40**, 40–55, 1975

Tolstoy, I.: Resonant frequencies and high modes in layered wave guides. J. Acoust. Soc. Am. **28**, 1182–1192, 1956

Tolstoy, I., Usdin, E.: Wave propagation in elastic plates: low and high mode dispersion. J. Acoust. Soc. Am. **29**, 37–42, 1957

Received April 12, 1985; revised version July 3, 1985
Accepted July 5, 1985